Cluster variational method for a fluid in a narrow capillary

E. Velasco and P. Tarazona
Departamento de Fisica de la Materia Condensada, C-XII, Universidad Autonoma de Madrid, Madrid E-28049, Spain
(Received 13 June 1990)

We present a theoretical study of a fluid in a narrow planar capillary, including the effects of the periodic structure of the confining walls. A layering transition had been observed for the same model in a previous Monte Carlo simulation, but it is missing in our density-functional calculation. The transition is recovered with an approach based on the cluster variational method, which treats the free energy as a functional of the four-particle distribution function.

I. INTRODUCTION

A fluid in a narrow capillary shows interesting differences with the behavior of a bulk system. The shift of the bulk liquid-vapor phase transition into the capillary condensation, already predicted by the macroscopic analysis of Kelvin and Laplace, has been studied with microscopic theories for lattice-gas and continuous models,[1] which can also account for the shift of the critical temperature. The crystallization of the fluid is also changed by the confinement; the competition between the intrinsic lattice parameter of the bulk crystal and the structure of the capillary wall may produce frustration, commensurate-incommensurate phases, and solid-fluid critical points, which make it an interesting but very difficult theoretical problem. Some attempts have been done with lattice-gas models,[2] but it is clear that a continuous description of the fluid is required to analyze the most interesting effects. The computer simulations have been mainly restricted to simplified models of a capillary with planar walls, neglecting the effects of the periodic structure of the wall at molecular scale.[3] This description may fail to describe the properties of very narrow capillaries, with a few molecular layers width, like expandable clays and other porous materials.[4] In these systems the periodic structure of the confining walls may be as important as the separation between the walls. The computer simulation of Schoen *et al.*[5] was directed to analyze these effects in a fluid with truncated Lennard-Jones (LJ) interactions inside a micropore made with two parallel (001) faces of a fcc crystal, also with LJ potentials. The system was studied along an isotherm path, changing the separation h between the two walls. The most interesting result was a sharp change in the structure of the system from a one-layer "liquid" phase for $h \leq 2.10$ to a two-layer "crystal" phase for $h \geq 2.15$, in LJ units.

Here we present a theoretical study of this system with several techniques. First with a density-functional approximation which had been successfully used in the study of wetting and drying transitions,[6] including the periodic corrugation of the walls. However, this approach fails to reproduce the layering transition in the capillary. Instead, there is a smooth evolution of the fluid structure from one layer to two layers. An exact analysis of the zero-temperature structure provides the clue of what is missing in the density-functional approximation and gives a possible alternative interpretation of the one-layer phase as the superposition of two asymmetric structures. To study these structures at finite temperature we include the correlation effects with a cluster variational theory for the distribution function of the molecules.

II. THE MODEL AND DENSITY-FUNCTIONAL APPROXIMATION

The micropore simulated by Schoen *et al.*[5] is made of two layers of atoms in a rigid two-dimensional (2D) square lattice with the two parallel walls out of phase, like consecutive (001) planes in a fcc lattice. The walls produce a confining potential acting on the fluid which is the sum of the LJ interactions:

$$V_w(r) = \sum_{\mathbf{R} \in \text{wall lattice}} \Phi(|r-R|) , \tag{2.1}$$

with the usual form for the LJ potential $\Phi(r)$ and the same LJ constants, ϵ and σ, as for the interaction between the molecules of the fluid (although the latter was truncated at $r = 2.5\sigma$). All the results here are expressed in reduced units of the LJ parameter $\epsilon/k_B = \sigma = 1$. The simulation was done at temperature $T = 1$ and wall lattice parameter a, equal to 1.13, with a few checks for larger a. It is worth noticing that the equilibrium value for the lattice constant of the fcc lattice with LJ interaction is $a = 1.09$, so that the simulated walls were more open than the equilibrium crystal surface for the same interactions. The grand-canonical Monte Carlo simulation was done along an isothermal path changing the wall separation from $h = 1.75$ to 6.20 at fixed value of $B = \mu - k_B T \ln(V)$, where V is the capillary volume. Here we shift the origin of the chemical potential to take out the thermal wavelength contribution, so that our μ corresponds to $\mu - k_B T \ln(\Lambda^3)$ in Ref. 5. The most interesting result was the sharp change of the total number of particles from $N = 57$ for $h = 2.10$ to $N = 98$ for $h = 2.15$, the number of LJ atoms in each wall being $N_s = 64$. The density profiles averaged over the xy directions parallel to the walls presented a sharp change from

one broad central layer at $h=2.10$ to two symmetric narrow peaks at $h=2.15$. The analysis of the transverse correlations lead the authors to interpret the monolayer phase as a fluid and the bilayers as a crystal. The density-functional approximation used here to study this system has been described in a previous work for the wetting and drying transitions[6] in a single wall and in a wide capillary, $h \geq 20$. The approximation is based on the separation of the LJ interactions into a hard-sphere (HS) core and the attractive interaction. The free energy of the HS is given by a nonlocal density functional which has been successfully used for several problems,[7,8] and the attractive interactions are included in an effective mean-field approximation. The full grand-potential energy, at fixed T and μ, is minimized with respect to the density distribution, $\rho(\mathbf{r})$, which is periodic in x and y, parallel to the walls, and vanishes for z out of a narrow interval, $0<z<h$. The details of the approximation and the numerical procedure are given in Ref. 6. In Fig. 1 we present the density distribution $\rho(z)$, averaged on x and y, which results of our calculation for $T=1$, $\mu=0$, and different capillary widths from $h=2.0$ to 2.7. It is clear that they correspond to a monolayer for small h and to a bilayer for the larger values of h, but the evolution from density distributions with a single central maximum to those with two symmetric maxima is smooth, without any signature of phase transition. The system with two layers, for $h=2.7$, may be regarded as a slab of the bulk crystal, but also as a fluid strongly modulated by the confining walls, with the same symmetry as the one-layer case. We have checked that the same qualitative behavior is observed at much lower temperatures, so that the failure to observe the layering transition is not a mere shift of the critical temperature due to our approximate density functional, but a qualitative defect of our approach. The failure of the density-functional calculation for this system should be contrasted with the qualitative and quantitative accuracy of the same approximation for the properties of a single interface, including the periodic structure of the wall[6] and for porous with parallel smooth walls.[8] The combined effects of the narrow confinement in the z direction and the periodic structure on the xy planes make it a more difficult and interesting problem to analyze.

III. ANALYSIS AT ZERO TEMPERATURE

The phase diagram in the (h,μ) plane for $T=0$ is given by the minima of the grand-potential energy:

$$\Omega=\frac{1}{2}\sum_{i\neq j=1}^{N}\Phi(|\mathbf{r}_i-\mathbf{r}_j|)+\sum_{i=1}^{N}V_w(\mathbf{r}_i)-\mu N \tag{3.1}$$

with respect to the number of molecules, N, and their positions $\mathbf{r}_i$ $(i=1,\ldots,N)$. In the range of capillary width studied here, there are three kinds of possible solutions: the empty capillary, $N=0$, the monolayer with as many molecules in the fluid as in each of the crystal walls, $N=N_s$, and the symmetric bilayer with $N=2N_s$. The position of the monolayer inside the capillary depends only on V_w, and it is straightforward to show that this function has two symmetric minima around the central value $z=h/2$, so that there are two degenerated monolayer phases. The symmetric central layer density profiles described in the computer simulation at $T=1$ are not present in the $T=0$ phase diagram. In the two-layer phase the two symmetric wells of V_w are occupied, although the position of the layers is shifted out of true minima of V_w by the layer-layer interaction. The phase diagram in the (h,μ) plane is obtained by direct comparison of the energy for each phase. The result is presented in Fig. 2. There is a triple point for $h_t=2.05$ and $\mu_t=-6.7$ at which the empty capillary [V (for vapor phase)], the symmetric bilayer (S_2), and the two asymmetric monolayers (A_1) coexist. For $h\geq h_t$ there is a direct transition from the V to the S_2 phase, while for $h<h_t$ there is a V-A_1 transition at low μ and a A_1-S_2 transition at a higher chemical potential. The diagram for very narrow capillaries ($h\lesssim 1.5$) shows some unrealistic features due to the model of the wall as a single layer with a lattice parameter larger than in the equilibrium crystal, but this is irrelevant for our discussion of the

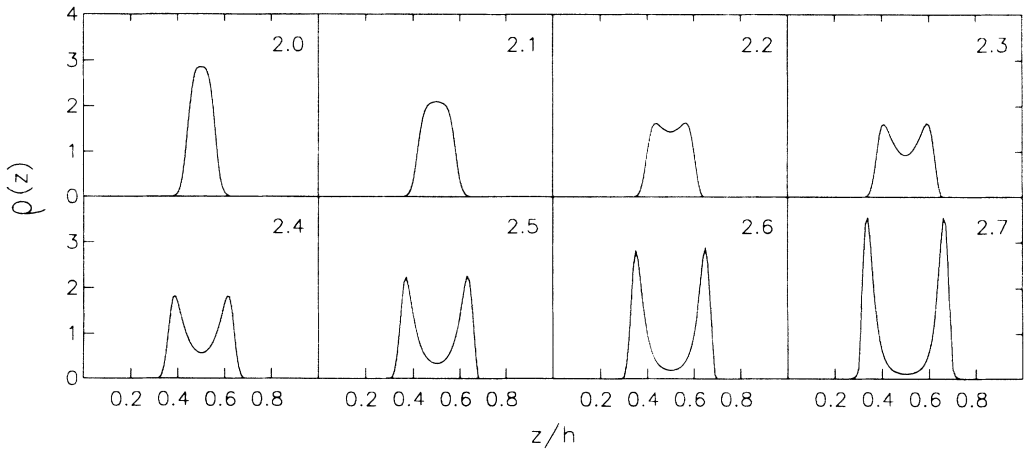

FIG. 1. Density profiles, averaged over the xy plane, as given by our density functional calculation for $T=1$, $\mu=0$ and different values of the capillary width h (given by the numbers from 2.0 to 2.7 inside the figures) showing the smooth evolution from one to two layers.

monolayer-bilayer transition. The conclusion of this analysis is that the symmetric monolayer is not present at $T=0$. Instead we have two degenerated phases, each one with a monolayer in an asymmetric position. These phases are found as global minima of the grand potential for $h \lesssim 2.05$, close to the location of the layering transition observed in the computer simulation.[5] The origin of these phases is the structure of the potential produced by the walls. As said above, the two walls would form the binary basis AB for the periodic structure $ABABAB\ldots$ of the (001) planes in a fcc lattice. The two walls with nothing in between would have the minimum energy for $h_0=2^{-1/2}$. The total energy would again be minimized for $h \simeq 3h_0$, with the capillary filled by two layers made of "fluid" atoms, making a $ABAB$ structure. However, to have a single layer of fluid in the capillary implies a stacking fault like AAB or ABB, which correspond to occupy each of the symmetric minima of V_w. The occupancy of both minima, to avoid the stacking fault, is penalized for $h \lesssim 2.24$ by the short-range repulsive interaction between the two "fluid" layers. This repulsion increases very fast as h decreases, so that the occupation of one of the two symmetric minima blockades the other and produces the asymmetric A_1 phases. In the density-functional approximation we have used a hard-sphere description of the core interactions instead of the soft repulsion of the original LJ interaction. With this approximation the effects described above should be enhanced because the double occupancy of the two wells would not only be penalized but completely forbidden for small h. However, this effect is missed by the density-functional approximation used to describe the hard-sphere fluid. This density functional uses the thermodynamics and correlation structure of the bulk fluid to describe, in an approximate way, the inhomogeneous system. The approximation is quite accurate for the layering of the fluid near a hard wall and also for the strong modulations in the crystal phase. However, this density functional, as any other analytic approximation based on the information of the bulk system, cannot take full account of the infinite repulsion between individual molecules. In particular, a density distribution with only two molecules separated by less than the HS diameter gives a large but finite free energy, instead of the infinite energy implied by the hard-sphere model. Moreover, the HS contribution to the free energy scales with k_BT, so that it disappears in the $T=0$ limit and the packing effects are missed altogether. A theoretical treatment of this problem should include the correlation structure in a consistent way, to avoid the partition of the interactions in a hard core and an attractive part. Only with this requirement may we get the correct $T=0$ limit and follow the evolution of the phase diagram to $T>0$. This is done in the next section with an approximation based on the cluster variational method.

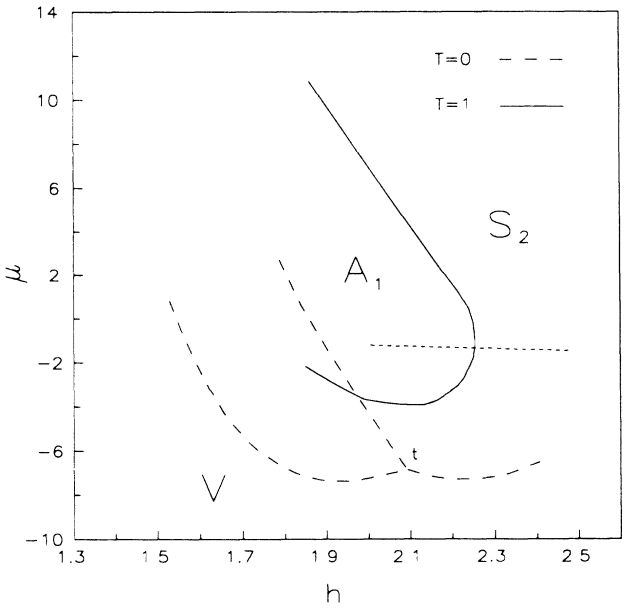

FIG. 2. Isotherm sections of the global phase diagram showing the stability regions of the different phases on the (μ,h) plane. For the $T=0$ isotherm there are three different phases in this interval of the capillary width h. The vapor phase (V) which represents the empty capillary at low chemical potential, the asymmetric monolayer A_1, and the symmetric bilayer S_2 are as described in the text. The three phases coexist at the triple point labeled as t. The $T=1$ isotherm has only two phases A_1 and S_2 because the V-S_2 transition has become critical below this temperature. The short-dashed line intersecting the $T=1$ coexistence isotherm represents the path followed by the computer simulation of Ref. 5.

IV. A CLUSTER VARIATIONAL APPROACH

The cluster variational method (CVM) was designed by Kikuchi *et al.*[9] and later developed also by other authors[10] as an approximation for lattice models. The method uses as a variable the probability of each possible configuration of a basic cluster of m lattice sites. The free energy of the system is written as a function of these probabilities, using a combination approximation for the entropy. By increasing the size of the basic cluster one may generate a series of approximations: the mean-field result corresponds to $m=1$ (the basic cluster being a single site), and the Bethe approximation is the $m=2$ case, with the nearest-neighbor bond as a basic cluster. If the lattice model has continuous variables, instead of a few possible values like in the Ising or Potts models, the probabilities of each configuration become continuous functions of the variables and the free energy is approximated by a functional of the m-site distribution function. The functional minimization leads to a set of integral equations which may be solved numerically. The method has proved to be useful for a system of planar rotors representing N_2 molecules adsorbed on graphite.[11] The application of the method to a fluid with continuous positions, without any real lattice, has been recently explored by Schlijper and Kikuchi,[12] but the power of the method in this case is still not clear. The problem we face here is different because although we want to treat the positions of the fluid molecules as continuous variables, our system has a real lattice structure, created by the potential of the capillary walls, which may be used to set the basic cluster in a natural way. We start by dividing the volume inside

the capillary into periodic cells containing one and only one of the minima of the wall potential, $V_w(\mathbf{r})$. On the xy planes we take the natural division given by the Wigner-Seitz two-dimensional unit cells of the square lattice. Along the z direction we just took the central plane $z=h/2$ as the boundary between the cells of each wall. The three-dimensional Wigner-Seitz cells of the two-wall lattice could appear as a more natural division, but it was more cumbersome to use and we do not expect important differences. For the range of h in which we are interested, two molecules in the same cell would have a very large potential energy, which would make these configurations very improbable at any reasonable value of T and μ. Thus, we may impose the restriction that any cell may be empty or be occupied by a single molecule. Each configuration of the basic cluster is fully described by the occupancy of each site, $n_i=0,1$ (the index i gives the position of the site) and by the position $\mathbf{r}_i$ of the molecule inside each occupied cell [in the following we use x_i as an abbreviation for $(n_i,\mathbf{r}_i)$]. We use a basic cluster with $m=4$ including two sites in each wall, as shown in Fig. 3. The interaction between the nearest-neighbor sites in the cluster is attractive for large h and becomes repulsive as h decreases, producing the blockade described above. The distribution function for the cluster formed by the sites i,j,k,l is given by the function $P_{i,j,k,l}(x,x',x'',x''')$. The distribution function for smaller clusters may be obtained from P_{ijkl} by integrating over part of the variables. Thus, the distribution function for the bond ij is given by

$$P_{i,j}(x,x')=\int_{x''}\int_{x'''}P_{i,j,k,l}(x,x',x'',x''') , \tag{4.1}$$

where we use an abbreviated form for the sum over $x=(n,\mathbf{r})$:

$$\int_x f(x)\equiv\int_x f(n,\mathbf{r})\equiv f(n=0)+\int_{\mathrm{UC}}d\mathbf{r}f(n=1,\mathbf{r}) , \tag{4.2}$$

where UC stands for the unit cell and we use that for $n=0$ any function of $x=(n,\mathbf{r})$ becomes independent of $\mathbf{r}$. The distribution function for one site is given by

$$P_i(x)=\int_x P_{i,j}(x,x') , \tag{4.3}$$

and the density distribution in each cell is given by

$$\rho_i(\mathbf{r})=P_i(n=1,\mathbf{r}) . \tag{4.4}$$

The total density distribution in our capillary is given by adding the contributions of each cell.

The distribution functions $P_{i,j,k,l}(x,x',x'',x''')$ have to be normalized:

$$\int_x\int_{x'}\int_{x''}\int_{x'''}P_{i,j,k,l}(x,x',x'',x''')=1 , \tag{4.5}$$

and through the relations (4.1)–(4.3) the normalization also applies to $P_{i,j}$ and P_i. In particular, the average number of molecules in the cell i is given by

$$N_i=\int_{\mathrm{UC}}d\mathbf{r}P_i(n=1,\mathbf{r})=1-P_i(n=0) . \tag{4.6}$$

The topology of our lattice is equivalent to the two-dimensional square lattice, in which nearest-neighbor sites are associated to the cells of opposite walls. The

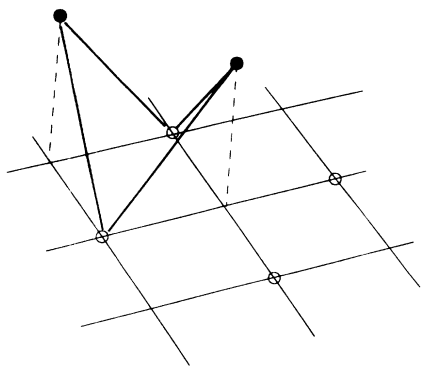

FIG. 3. Sketch of the basic cluster used in the CVM. The open circles on a square lattice represent the center of the unit cells associated to one of the walls. The solid circles are the centers of the unit cells associated to the other wall; they are also in a square lattice, although we have represented here only two of them. The two square lattices are displaced with respect to each other. The solid lines join the solid circles to their nearest-neighbor open circles in the basic cluster of our sites. The full system may be filled with these basic clusters sharing bonds, with the same topology as the square lattice.

CVM applied to this lattice with $m=4$ corresponds to the Kramers-Wannier approximation for the Ising model in the square lattice. With the notation (4.2) we write the grand-potential energy as

$$\begin{aligned}\Omega=&\sum_{(i,j,k,l)}k_BT\int_x\int_{x'}\int_{x''}\int_{x'''}P_{i,j,k,l}\ln(P_{i,j,k,l})\\&-\sum_{(i,j)}\int_x\int_{x'}P_{i,j}[k_BT\ln(P_{i,j})-n_in_j\Phi(|\mathbf{r}_i-\mathbf{r}_j|)]\\&+\sum_{(i)}\int_x P_i\{k_BT\ln(P_i)+n_i[V_w(\mathbf{r}_i)-\mu]\} ,\end{aligned} \tag{4.7}$$

where the sum over (i,j,k,l) runs over all the basic clusters in the lattice, the sum over (i,j) runs over all the nearest-neighbor pairs, and that on (i) over all the lattice sites. This expression has to be minimized with respect to the functions $P_{i,j,k,l}$ with the constraints that the bond distribution functions should give the same result when evaluated from the two clusters sharing the same bond. These constraints may be imposed with the appropriate Lagrange multipliers (as done in Ref. 11) so that at the end we reduce the problem to the minimization with respect to a single basic cluster, say $P_{1,2,3,4}$, and it may be written in terms of the two-site distribution functions $P_{i,j}$ and a set of two-site Lagrange multipliers $A_{i,j}(x,x')$ (with $i,j=1-4$):

$$\begin{aligned}&P_{1,2,3,4}(x,x',x'',x''')\\&\quad=CY_{1,2}(x,x')Y_{2,3}(x',x'')Y_{3,4}(x'',x''')Y_{4,1}(x''',x) ,\end{aligned} \tag{4.8}$$

where C is a normalization constant fixed to satisfy (4.5) and

$$Y_{i,j}(x,x') \equiv \left[\frac{P_{i,j}(x,x') A_{i,j}(x,x') \exp[-n_i n_j \Phi(|\mathbf{r}_i - \mathbf{r}_j|)/(k_B T)]}{[P_i(x) P_j(x')]^{1/4}} \right]^{1/2} . \quad (4.9)$$

From (4.1) and (4.8) we get the following set of coupled integral equations for $P_{i,j}$ and $A_{i,j}$:

$$P_{i,j}(x,x') = C Y_{i,j}(x,x') T_{i,j}(x,x') \quad (4.10)$$

and

$$A_{i,j}(x,x') = \frac{T_{j,k}(R(x),R(x'))}{T_{i,j}(x,x')} , \quad (4.11)$$

where

$$T_{i,j}(x,x') \equiv \int_{x''} \int_{x'''} Y_{j,k}(x',x'') Y_{k,l}(x'',x''') Y_{l,i}(x''',x) , \quad (4.12)$$

and where indices i,j,k,l run on cycles over 1,2,3,4; R, in (4.11), is the rotation operator that transforms $\mathbf{r}=(x,y,z)$ into $R(\mathbf{r})=(y,-x,z)$.

At $T=0$ the contribution of the entropy to (4.7) vanishes and we are left with the exact phase diagram of Sec. III. For $T>0$ our expression for the entropy is only approximate but we hope relatively accurate, because we are including the main effects of the correlation up to the four-nearest-neighbor term of the basic cluster. The numerical integration over the cells adds some uncertainty to the quantitative accuracy of our predictions, but with a judicious use of special quadratures we may get them with a reduced number of points. The integral equations are solved by iterations with good convergence from an appropriate initial guess.

V. RESULTS AND DISCUSSION

The iterative scheme used to solve the integral equations of the CVM keeps the symmetry of the initial guess for the pair distribution functions. Phases like the S_2 and V of the $T=0$ phase diagram are obtained from a symmetric input with nearly full or nearly empty capillaries. The asymmetric phases A_1 can also be obtained if we start with an asymmetric distribution function. At low temperature we obtain all the phases of the $T=0$ diagram, although the phases boundaries in the (h,μ) diagram are shifted with T. The direct transition from V (the low-density vapor phase which is vacuum at $T=0$) to S_2 (the bilayer solid), at $h \gtrsim 2.05$, becomes weaker with increasing T up to a critical temperature depending on $h, T_c(h)$, at which the phase transition disappears. We have followed this in detail for $h=2,3$, and the results for the total number of molecules in the capillary as a function of the chemical potential for different isotherms are presented in Fig. 4. The critical temperature for this value of h is about $T_c=0.48$, so that the transition cannot be observed in the simulation of Ref. 5, done at $T=1$. The existence of a critical temperature for the V-S_2 transition and the smooth evolution of the density distribution for $T \geq T_c(h)$ is possible because the S_2 phase has not broken any symmetry of the wall potential; it may be regarded as a "crystal" phase because the density distribution is made of narrow peaks in the regular positions of the V_w minima, but it has the same symmetry as the V phase, which is regarded as a rarified fluid modulated by the wall potential. In this respect the asymmetric phases are different; they have a broken symmetry which makes them qualitatively different from the other phases.

The V-A_1 and A_1-S_2 coexistence lines at $T>0$ are also shifted with respect to the $T=0$ phase diagram. The main effect can be understood in terms of the entropic contribution to the free energy. The monolayers in the A_1 phases are at the minima of the wall potential, which has relatively wide wells. At finite T we expect that the fluid molecules would be vibrating around the minima, giving a density distribution made of relatively wide peaks. In the S_2 phase, for narrow capillaries, the double occupancy of the potential wells includes a repulsive term

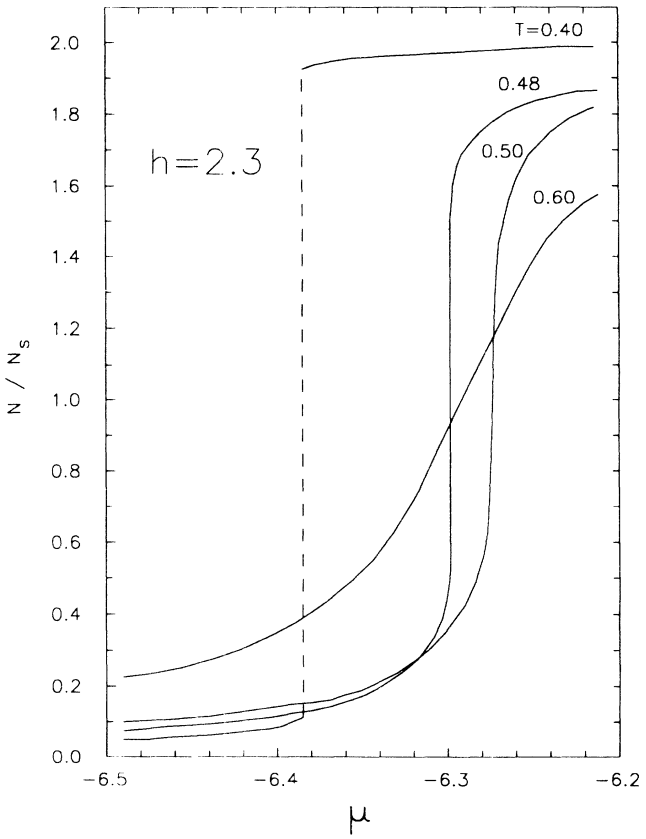

FIG. 4. The number of molecules in the capillary as function of the chemical potential for different temperatures at fixed capillary width $h=2.3$. At low temperature there is a phase transition from the V phase, $N/N_s \ll 1$, to the bilayer S_2, with N/N_s close to 2. The transition becomes critical at $T=0.48$ (for this particular value of h) and above this temperature the system goes smoothly from the empty capillary to the bilayer.

between the nearest-neighbor molecules which pushes them against the walls, the effective potential has minima which are much narrower than those of V_w, and the peaks of the density distribution in this phase are much sharper than in the A_1 phase. This argument is valid for $h \lesssim 2.2$, so that for these values of h the entropy is greater in the A_1 than in the S_2 phase, and the first one should become relatively more stable as T increases. The second change we may expect with respect to the $T=0$ phase diagram is that when the critical temperature for the V-S_2 phase coincides with the triple V-A_1-S_2 coexistence, the differences between the V and the S_2 disappear, and we should find a single boundary between the asymmetric and the symmetric phases in the (μ,h) phase diagram. At $T=1$, the temperature studied in the computer simulation,[5] the phase diagram (Fig. 2) shows the stable A_1 phases for $h \leq 2.15$ and intermediate values of the chemical potential. The isothermal path followed in the computer simulation corresponds to a chemical potential decreasing with increasing h as

$$\mu = 3.5 - \ln(s^2 h) , \tag{5.1}$$

where $s=7.9925$ is the linear size of the simulation box in the xy plane. In the scale of Fig. 2 this path is nearly horizontal from $\mu=1.21$ at $h=2$ to $\mu=-1.53$ at $h=2.4$. Our prediction along this path is a transition between $h=2.15$ and 2.20 from the asymmetric phase for small h to the (supercritical) symmetric phase at large h. This corresponds exactly to the location of the transition from the bilayer "crystal" to the monolayer "fluid" observed in the simulation. However, our calculation indicates the stability of the asymmetric monolayer with respect to the symmetric monolayer, which can also be obtained as an unstable solution of the CVM equations, by iterating from initial symmetric distribution functions. Of course, at high temperature we should recover a density distribution with the full symmetry of the wall potential, and with adequate tuning of h and μ we can always find a stable symmetric monolayer phase. To check the transition from the asymmetric to the symmetric monolayer, we have performed a series of calculations at fixed $h=2.1$ and $\mu=-1.5$ with increasing temperature. The result is a smooth change from the asymmetric to the symmetric phase, with N/N_s nearly equal to 1, between $T=1.6$ and 1.7, well above the temperature of the simulation.[5]

In conclusion, the capillary model simulated by Schoen *et al.*[5] is a particularly hard test for theoretical approximations. Our density-functional approach, which had been successfully used to describe the properties of single walls and smooth capillaries, fails to reproduce the behavior of these systems, due to the combined effects of the narrow confinement and the structure of the walls. The phase diagram for this system at $T=0$ shows the existence of asymmetric monolayers in a finite interval of μ for $h \lesssim 2.05$. We have obtained the phase diagram at $T>0$ with a CVM calculation in which the free energy is written as a functional of the four-molecule distribution function. With this approach we reproduced the monolayer-bilayer transition observed in the simulation at $T=1$ between $h=2.15$ and 2.2, but our monolayer phase is asymmetric. A possible interpretation of this result is that a symmetric monolayer density profile may be obtained by superimposing the two degenerated asymmetric phases, which corresponds to having the capillary filled with a mixture of the "right" and "left" monolayers. This produces the symmetric density distributions, averaged over the xy plane, shown in Fig. 5 which is qualitatively similar to those observed in the simulation. Such superposition of the two degenerated asymmetric phases may appear in the computer simulation, and the long-run averages would show symmetric monolayers. Otherwise, the discrepancy may be a defect of our theoretical approach, which may be overestimating the stability of the asymmetric monolayer with respect to the symmetric one. However, we are sure of the existence of the A_1 phases in the $T=0$ phase diagram, and they should still be there at finite but small T. Our estimate of $T=1.7$ for the end of the stability of the asymmetric phase may be too high, but the accuracy of the CVM with $m=4$ to predict the critical temperatures for other models within a few percent error makes unlikely such a gross overestimation.

Finally, we have to remark that the richness of the phase diagram and the difficulty of its theoretical study are partially produced by the choice of antisymmetric walls. As described above, the capillary walls are two consecutive (001) planes in a fcc crystal. The capillary width is changed by moving the planes away from each other along the z direction without any displacement on the xy plane. Thus, the capillary has the symmetry to accommodate an even number of layers but it leads to stacking-fault defects, with breaking of the symmetry, if we try to put an odd number of layers. These defects

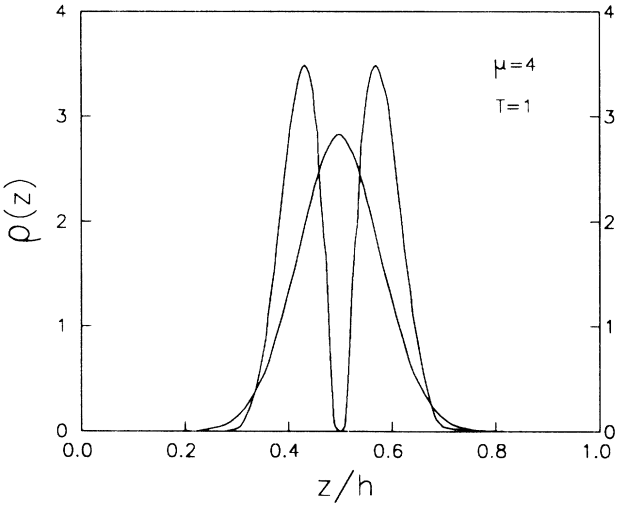

FIG. 5. Density profiles, averaged over the xy plane calculated with the CVM across the A_1-S_2 transition for $T=1$ and $\mu=4$. The profile with two peaks corresponds to the bilayer S_2 for $h=2.2$ and the profile with the single central maximum is obtained as the superposition of the two asymmetric monolayers A_1 for $h=2.0$. The result of this superposition is the broad central maximum qualitatively similar to those observed in the computer simulation of Ref. 5.

might be easily healed by allowing the walls to make a relative displacement on the xy plane so as to become symmetric or antisymmetric depending on the number of fluid layers which can be accommodated in the capillary. In that case, all the phases would have the full symmetry of the wall potential. That may be the relevant model for expandable clays if we imagine them as being made of silicate sheets bonded together by molecular forces, but with the ability to slip over their neighbor, at least over molecular distances, to better accommodate a monolayer of water (with the due apologies for neglecting the peculiarities of the water interaction potential).

ACKNOWLEDGMENTS

This work has been financed by the Direccion General de Investigacion Científica y Técnica of Spain (SEUI Grant No. PB0237).

[1]M. E. Fisher and H. Nakanishi, J. Chem. Phys. **75**, 5857 (1981); B. C. Freasier and S. Nordholm, *ibid.* **79**, 4431 (1983); R. Evans and P. Tarazona, Phys. Rev. Lett. **52**, 557 (1984), E. Bruno, U. Marini Bettolo Marconi, and R. Evans, Physica A **141**, 187 (1987).

[2]P. Tarazona and L. Vicente, Mol. Phys. **56**, 557 (1985); G. Navascues and P. Tarazona, *ibid.* **62**, 497-507 (1987).

[3]L. A. Rowley, D. Nicholson, and N. G. Parsonage, Mol. Phys. **31**, 365 (1976); **31**, 389 (1976); J. E. Lane and T. H. Spurling, Chem. Phys. Lett. **67**, 107 (1979); Aust. J. Chem. **29**, 2103 (1976); F. F. Abraham, J. Chem. Phys. **68**, 3713 (1979); I. K. Snook and W. van Mergen, *ibid.* **72**, 2907 (1980).

[4]See, e.g., R. M. Barrer, Philos. Trans. R. Soc. London Ser. A **311**, 333 (1984).

[5]M. Schoen, D. J. Diestler, and J. H. Cushman, J. Chem. Phys. **87**, 5464 (1987).

[6]E. Velasco and P. Tarazona, J. Chem. Phys. **91**, 7916 (1989).

[7]P. Tarazona, Phys. Rev. A **31**, 2672 (1985).

[8]P. Tarazona, U. Marini Bettolo Marconi, and R. Evans, Mol. Phys. **60**, 573 (1987); P. C. Ball and R. Evans, *ibid.* **63**, 159 (1988).

[9]R. Kikuchi, Phys. Rev. **81**, 988 (1951); M. Kurata and R. Kikuchi, J. Chem. Phys. **21**, 434 (1953); R. Kikuchi and S. G. Brush, *ibid.* **47**, 197 (1967).

[10]See, e.g., A. Surda, Z. Phys. B **46**, 371 (1982); A. G. Shijper, J. Stat. Phys. **40**, 1 (1985), and references therein.

[11]E. Chacon and P. Tarazona, Phys. Rev. B **39**, 7111 (1989).

[12]A. G. Schlijper and R. Kikuchi (unpublished).